http://www.kidney-international.org

OPEN

see commentary on page 5

Establishing 3-nitrotyrosine as a biomarker for the vasculopathy of Fabry disease

Liming Shu[1], Anuradha Vivekanandan-Giri[1], Subramaniam Pennathur[1], Bouwien E. Smid[2], Johannes M.F.G Aerts[3], Carla E.M. Hollak[2] and James A. Shayman[1]

[1]*Department of Internal Medicine, University of Michigan, Ann Arbor, Michigan, USA;* [2]*Department of Endocrinology and Metabolism, Academic Medical Centre, Amsterdam, The Netherlands and* [3]*Department of Medical Biochemistry, Academic Medical Centre, Amsterdam, The Netherlands*

The endothelial dysfunction of Fabry disease results from α-galactosidase A deficiency leading to the accumulation of globotriaosylceramide. Vasculopathy in the α-galactosidase A null mouse is manifested as oxidant-induced thrombosis, accelerated atherogenesis, and impaired arterial reactivity. To better understand the pathogenesis of Fabry disease in humans, we generated a human cell model by using RNA interference. Hybrid endothelial cells were transiently transfected with small interfering RNA (siRNA) specifically directed against α-galactosidase A. Knockdown of α-galactosidase A was confirmed using immunoblotting and globotriaosylceramide accumulation. Endothelial nitric oxide synthase (eNOS) activity was correspondingly decreased by >60%. Levels of 3-nitrotyrosine (3NT), a specific marker for reactive nitrogen species and quantified using mass spectrometry, increased by 40- to 120-fold without corresponding changes in other oxidized amino acids, consistent with eNOS-derived reactive nitrogen species as the source of the reactive oxygen species. eNOS uncoupling was confirmed by the observed increase in free plasma and protein-bound aortic 3NT levels in the α-galactosidase A knockout mice. Finally, 3NT levels, assayed in biobanked plasma samples from patients with classical Fabry disease, were over sixfold elevated compared with age- and gender-matched controls. Thus, 3NT may serve as a biomarker for the vascular involvement in Fabry disease.

Kidney International (2014) **86,** 58–66; doi:10.1038/ki.2013.520; published online 8 January 2014

KEYWORDS: endothelial cell; endothelial nitric oxide synthase; Fabry disease; globotriaosylceramide

Correspondence: *James A. Shayman, Department of Internal Medicine, 1150 West Medical Center Drive, Ann Arbor, Michigan 48109-0676, USA. E-mail: jshayman@umich.edu*

Received 18 March 2013; revised 4 November 2013; accepted 14 November 2013; published online 8 January 2014

Fabry disease (FD) is an X-linked lysosomal storage disease arising from a deficiency in α-galactosidase A (GLA). A loss of GLA activity results in the accumulation of glycosphingolipids with galα-1,4 gal linkages including globotriaosylceramide (Gb3), galabiosylceramide, and globotriaosylsphingosine (lyso-Gb3). FD has a pleiotropic phenotype that includes renal disease, cardiomyopathy, and vasculopathy. The vasculopathy is the basis for the life-threatening complications of FD, including stroke, hypertrophic cardiomyopathy, and renal failure. Whereas enzyme replacement therapy with recombinant GLA has emerged as a therapeutic option for FD, its effectiveness in preventing the long-term cardiovascular morbidities has been questioned.[1] The ability to evaluate and deliver effective therapy is limited by a poor understanding of the pathogenesis of the vasculopathy and by the absence of a biomarker that corresponds directly with the presence and degree of vascular dysfunction.

The Gla null mouse has been an useful model from exploring the vascular pathophysiology of FD. Although this mouse does not exhibit a spontaneous vascular phenotype, several inducible models of vascular disease have been reported. These include oxidant-induced thrombosis,[2] accelerated atherogenesis,[3] and impaired vasorelaxation.[4] A common mechanism that could potentially link these experimentally observed abnormalities is endothelial nitric oxide synthase (eNOS) dysfunction.[5] eNOS dysfunction may result in either decreased nitric oxide (NO) bioavailability or enzyme uncoupling, which generates a potent oxidant, peroxynitrite, a reactive nitrogen species.[6,7] The relationship between GLA and eNOS was explored by determining whether these changes could be recapitulated in a human endothelial cell line. We report that when the Gb3 content of EA.hy926 cells is increased with GLA knockdown, there is an associated uncoupling of eNOS with the formation of 3-nitrotyrosine (3NT), a specific marker for reactive nitrogen species. The eNOS dysfunction was specifically associated with the loss of GLA activity in that comparable changes were not observed with β-glucocerebrosidase (GBA) knockdown. High circulating levels of 3NT were measured in the plasma and aortic extracts of Gla knockout mice.

Finally, the concentrations of protein-bound oxidized amino acids were measured in plasma samples from classic

FD patients and compared with age- and gender-matched controls. A more than fivefold elevation in 3NT was observed in the FD samples compared with controls, raising the possibility that 3NT represents an useful biomarker for vasculopathy in FD.

RESULTS

EA.hy926 cell studies

Previous work in GLA-deficient mice demonstrated endothelial dysfunction associated with decreased NO bioavailability and eNOS uncoupling.[5] To determine whether similar abnormalities could be documented in a human vascular endothelial cell line, immortalized EA.hy926 cells, derived from fused HUVEC and A549 cells, were employed. EA.hy926 cells retain endothelial characteristics, including Factor VIII-related antigen expression, eNOS gene expression, and Weibel–Palade bodies.[8,9] Importantly, EA.hy926 cells also are characterized by measureable Gb3 and GLA (Figure 1a and b).

The silencing efficacies of Dicer-substrate RNAs (dsiRNA) (27-mer) and traditional small interfering RNA (siRNA) (21-mer) were assessed to determine whether it would be possible to fully suppress the expression and activity of GLA in cultured EA.hy926 cells. The conventional 21-mer siRNA against human GLA demonstrated low efficiency and short blocking times (data not shown). By contrast, anti-human GLA-dsiRNA completely knocked down GLA in cultured EA.hy926 cells for up to 3 days at a relatively low siRNA concentration (10 nM) as confirmed using immunoblotting (Figure 1a). As both siRNA and dsiRNA interference are transient, a second transfection was performed 3 days later. Under these conditions, GLA silencing was observed up to day 6. The lower expression of GLA was associated with the accumulation of Gb3 (Figure 1b). A correlation between increased Gb3 and the degree of GLA knockdown was observed. Compared with control-dsiRNA–transfected cells, the Gb3 levels in GLA-dsiRNA–transfected cells increased with the duration of the incubation with GLA-dsiRNA, ranging from 210% of control on day 2 after a single transfection up to 275% on day 6 with a double transfection (Figure 1c).

The specificity of the Gb3 changes was evaluated by use of GBA-dsiRNA. *GBA* encodes β-glucocerebrosidase, the lysosomal glycosidase that degrades glucosylceramide (GlcCer) to ceramide. GBA expression in cultured EA.hy926 cells was suppressed to undetectable levels. The silencing effect lasted until day 6 as measured using immunoblotting (Figure 2a). This silencing effect was observed following both single transfection and double transfection with the 27-mer anti-human GBA-dsiRNA. The corresponding loss of GBA activity resulted in the accumulation of GlcCer (Figure 2b). The specificity of this effect was demonstrated by the absence of any corresponding change in galactosylceramide, a cerebroside that is not a substrate for GlcCerase.

GlcCer mass increased fivefold in GBA-dsiRNA–transfected cells relative to the levels in control-dsiRNA cells

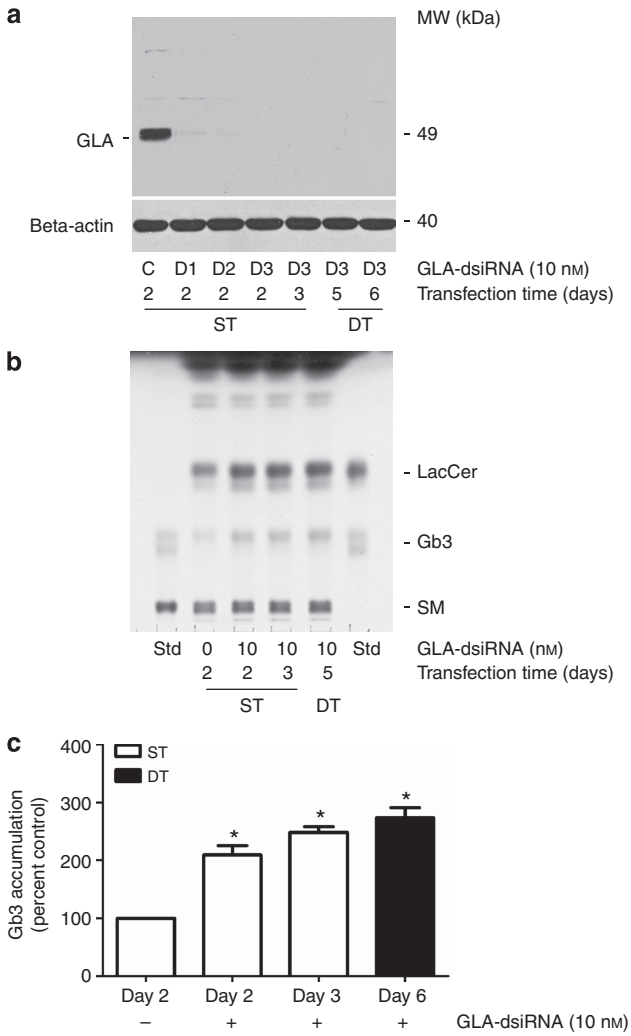

Figure 1 | Alpha-galactosidase A (GLA) knockdown raises globotriaosylceramide (Gb3) in a time-dependent manner. (**a**) A representative immunoblot for complete knockdown of the GLA from cultured EA.hy926 cells by three anti-human GLA-dsiRNA (Dicer-substrate RNA) duplexes (D1, D2, D3) at the indicated exposure times. (**b**) A representative thin layer chromatogram of neutral sphingolipids demonstrating Gb3 accumulation in GLA-dsiRNA–transfected EA.hy926 cells harvested on days 2 and 3 after a single transfection (ST) and on day 5 and 6 after double transfections (DT), respectively. LacCer, lactosylceramide; SM, sphingomyelin; Std., standards. (**c**) Gb3 levels in EA.hy926 cells as determined by scanning densitometry with the ImageJ software (NIH, Bethesda, MD). The values were normalized to Gb3 levels in cells transfected with a non-targeting control-dsiRNA. The data represent the mean ± s.e. from six independent experiments. *$P < 0.01$.

(Figure 2c). A small but reproducible reduction in GlcCer from its peak level occurred on day 4 after first transfection likely due to transient effect of siRNA. When a double GBA-dsiRNA transfection was performed, the cellular GlcCer levels on day 6 were as high as those observed on day 3 with a single transfection (Figure 2c). Although GlcCer is a precursor in Gb3 synthesis, no increase in Gb3 levels were observed in cells subjected to GBA-dsiRNA transfection (Figure 2d and e).

Glyceraldehyde 3-phosphate dehydrogenase (GAPDH) was silenced with GAPDH-dsiRNA to evaluate the effects of transfection on endothelial cell phenotype, morphology, oxidant stress, and viability because of either nonspecific or specific gene knockdown. GAPDH expression in EA.hy926 cells was lowered >98% by GAPDH-dsiRNA as measured using immunoblotting. A double transfection enhanced and prolonged the interference of GAPDH expression up to 6 days (Figure 3a). Cell numbers and viability following transfections were measured daily. The growth curve showed a similar recovery and growth pattern in cells transfected with control, GBA, and GAPDH-dsiRNAs. However, GLA-dsiRNA transfection was associated with lower growth and increased cell detachment from cultured dishes (Figure 3b). Forty percent of the detached cells remained viable and metabolically active as measured by trypan blue exclusion.

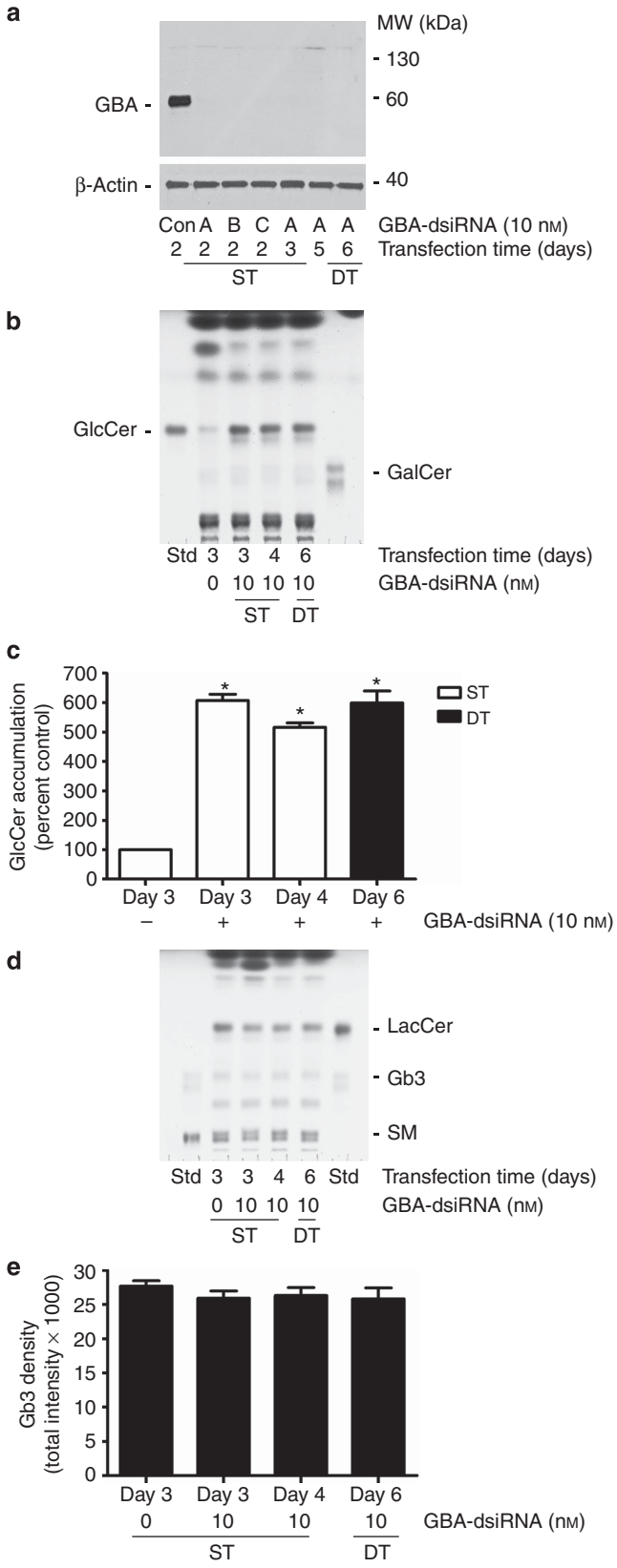

Figure 2 | β-Glucocerebrosidase knockdown does not raise globotriaosylceramide (Gb3). (**a**) Knockdown of the *GBA* (β-glucocerebrosidase) gene and suppression of β-glucocerebrosidase, another lysosomal hydrolase, in cultured EA.hy926 cells by three duplexes of anti-human GBA-dsiRNA (Dicer-substrate RNA) (A, B, and C) at the indicated exposure times as confirmed using immune bot analysis. (**b**) Lipids analysis of the glucosylceramide (GlcCer) levels in control-dsiRNA and GBA-dsiRNA–transfected EA.hy926 cells on days 3 and 4 of following a single transfection (ST) and on day 6 following a double transfection (DT). GalCer, galactosylceramide; Std., standards. (**c**) Determination of GlcCer accumulation in control- and GBA-dsiRNA–transfected cells by densitometric scanning ($n = 3$). (**d**) Levels of Gb3 in GBA–siRNA-transfected cells assessed in parallel using high-performance thin layer chromatography, and (**e**) as determined using scanning densitometry ($n = 3$). The error bars represent ± s.e. *$P < 0.01$.

Gla knockout mouse studies

Previous investigations uncovered the high levels of 3NT and *ortho*-tyrosine formation in mouse aortic endothelial cells isolated from Fabry mice, demonstrating that oxidant stress is characteristic of the Fabry mouse aortic endothelial cell phenotype.[5] The levels of protein-bound oxidatively modified amino acids were quantified using tandem mass spectrometry in cultured EA.hy926 cells transfected with GLA-dsiRNA (Gene 1), GBA-dsiRNA (Gene 2), and GAPDH-dsiRNA (Gene 3), respectively. Low levels were detectable in control-dsiRNA–transfected EA.hy926 cells and served as basal levels. 3NT, a specific marker for reactive nitrogen species, was markedly elevated (40- to 120-fold) in GLA-dsiRNA–transfected cells (Figure 4a) without corresponding changes in other oxidized tyrosines, including 3-chlorotyrosine, *ortho*-tyrosine, *meta*-tyrosine, and *o,o′*-dityrosine (Figure 4b), consistent with the mouse model of FD.[5] Double GBA-dsiRNA transfection modestly increased 3NT formation. However, this change was not associated with Gb3 accumulation in that GBA-dsiRNA transfection did not raise Gb3 under any conditions (Figure 2d and e), and also not related with repeated siRNA reagents usage, as double GAPDH-dsiRNA transfection did not increase nitrotyrosine production compared with that in single GAPDH-dsiRNA–transfected EA.hy926 cells (Figure 4a).

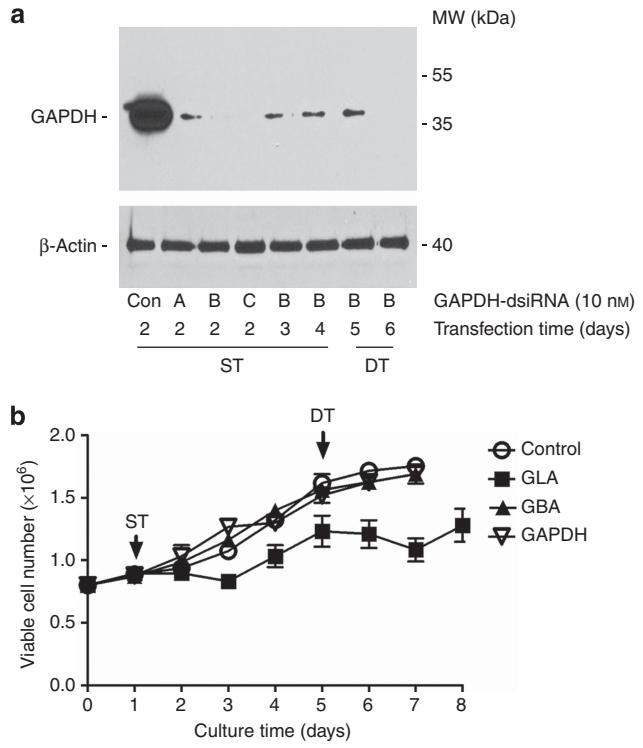

Figure 3 | Interference of glyceraldehyde 3-phosphate dehydrogenase (GAPDH) expression and effect on cell viability in transfected cells. (**a**) EA.hy926 cells were transfected with three anti-human GAPDH-dsiRNA (Dicer-substrate RNA) duplexes (A, B, and C) at indicated concentration for indicated days. Harvested cells were lysed in 1% Triton X-100 lysate buffer and analyzed using western blot. Upper panel, a representative immunoblot of GAPDH knockdown in cultured EA.hy926 cells. Lower panel, immunoblot for β-actin. (**b**) The number of viable transfected EA.hy926 cells were counted and recorded daily based on trypan blue exclusion. All experiments were repeated for three times with three different batches of cell cultures under similar conditions. ST, single transfection; DT, double transfection.

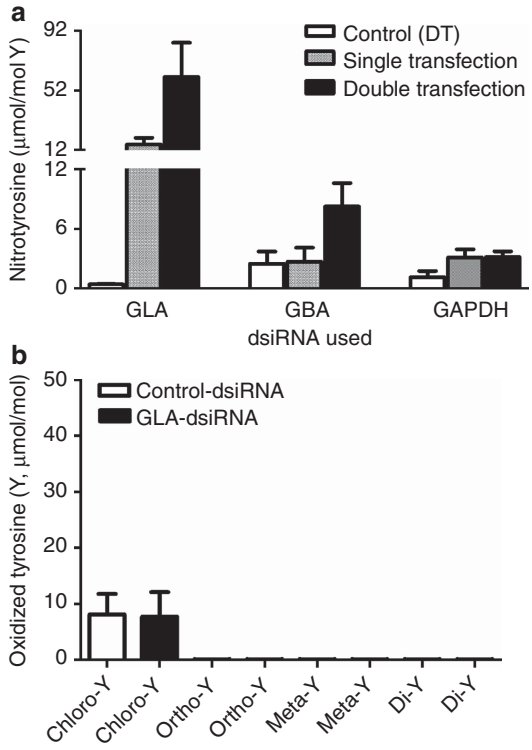

Figure 4 | Oxidant stress is characteristic of the Fabry human endothelial cell phenotype. (**a**) Comparison of nitrotyrosine content in cultured EA.hy926 cells transfected, respectively, with GLA (alpha-galactosidase A)–dsiRNA (Dicer-substrate RNA) ($n = 4$), GBA (β-glucocerebrosidase)-dsiRNA ($n = 4$), and GAPDH (glyceraldehyde 3-phosphate dehydrogenase)–dsiRNA ($n = 3$) as measured using liquid chromatography–electrospray ionization tandem mass spectrometry (LC/ESI/MS). The results were normalized to the protein content of tyrosine, the precursor of 3-nitrotyrosine. (**b**) Levels of other oxidant amino acids; chlorotyrosine (Chloro-Y), ortho-tyrosine (Ortho-Y), meta-tyrosine (Meta-Y), and dityrosine (Di-Y) in endothelial cells transfected twice with either control-dsiRNA or GLA-dsiRNA as analyzed using LCE-ITMS ($n = 3$).

eNOS activity was next measured in GLA-dsiRNA–transfected cells. As shown in Figure 5a, eNOS activity correspondingly decreased in the EA.hy926 cells, and the reduction was >60% on day 3 following the first GLA-dsiRNA transfection and >90% on day 6 following the second GLA-dsiRNA transfection. No difference was found in GBA- and GAPDH-dsiRNA–transfected cells with control-dsiRNA–transected cells (Figure 5b), consistent with a specific effect of Gb3 accumulation on eNOS activity.

3NT levels in plasma samples were measured using mass spectrometry in the GLA knockout mouse. A statistically significant increase in 3NT formation (100% vs. 171%) was observed between 2-month-old wild-type and Gla-/0 mice (Figure 6). A more significant elevation of nitrotyrosine (431%) in 9-month-old Gla-/0 mice was measured compared with wild-type mice at the same age, consistent with the age-dependent accumulation of Gb3 in the vasculature. Nine-month-old wild-type mice had a 45% higher level of nitrotyrosine in the plasma than their 2-month-old counterparts.

Protein modification by nitration of tyrosine to 3NT has been correlated with elevated oxidative stress.[10] Immunoblots of aortic homogenates demonstrated higher levels of 3NT in aortas dissected from Gla null compared with wild-type mice at 2 and 8 months of age (Figure 7a). A sixfold increase in 3NT formation in the older Gla null mouse aortas compared with wild-type aortas was confirmed using scanning densitometry (Figure 7b).

3-Nitrotyrosine measurements in Fabry patients

Biobanked plasma samples from 13 male Fabry patients were analyzed for oxidized amino acids including 3NT and compared with 11 control samples that were age- and gender-matched from the same biobank. Affected patients had classical symptoms of FD including acroparasthesias, cornea verticillata, and angiokeratomas in association with low or absent GLA activity, increased levels of plasma Gb3, and high concentrations of plasma lyso-Gb3 (Table 1).

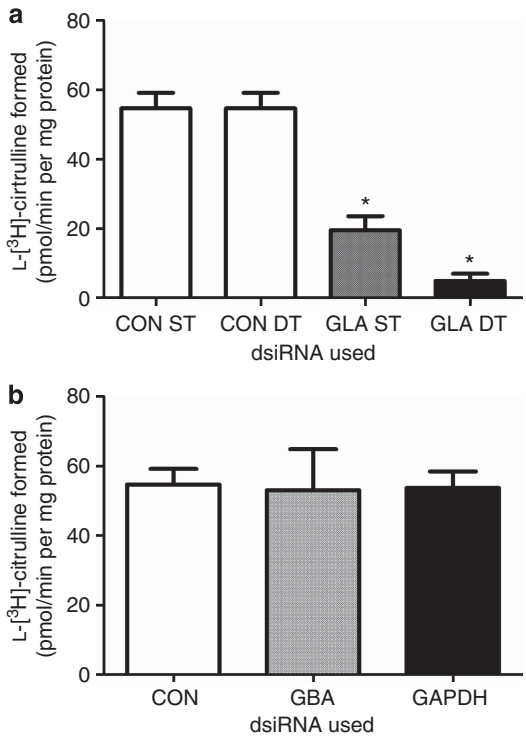

Figure 5 | Reduction of endothelial nitric oxide synthase (eNOS) activity in transfected EA.hy926 cells. (**a**) The cellular activities of eNOS in cultured human endothelial EA.hy926 cells transfected with either control–dsiRNA (Dicer-substrate RNA) or GLA (alpha-galactosidase A)-dsiRNA were measured based on the biochemical conversion of [^{3}H]L-citrulline from [^{3}H]L-arginine in intact cells. The experiments were performed on day 3 following single GLA-dsiRNA transfection (ST) and day 6 following double GLA-dsiRNA transfection (DT), respectively. (**b**) Comparison of eNOS activity in GBA (β-glucocerebrosidase)-dsiRNA and GAPDH (glyceraldehyde 3-phosphate dehydrogenase)-dsiRNA-transfected EA.hy926 cells to control-dsiRNA–transfected cells. The experiments were carried on day 6 following double transfections (DT). The enzyme activity was normalized to protein concentration and expressed as pmol/min per mg protein ($n = 4$). *$P < 0.01$.

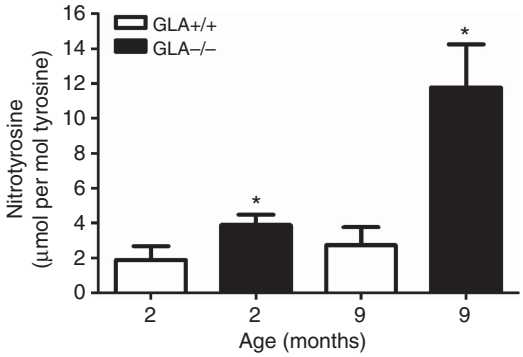

Figure 6 | Elevation of free 3-nitrotyrosine in wild-type and Gla (alpha-galactosidase A) null mouse plasma. Mouse blood was collected from the retro-orbital plexes of 2- and 9-month-old wild type and Gla null mice, respectively, as described in 'Materials and Methods'. The nitrated tyrosine in plasma was measured using LC/ESI/MS. The results were normalized to the tyrosine content, the precursor of 3-nitrotyrosine (3NT). The experiment was conducted twice and performed in triplicate. Values are means ± s.e. ($n = 6$). *$P < 0.01$.

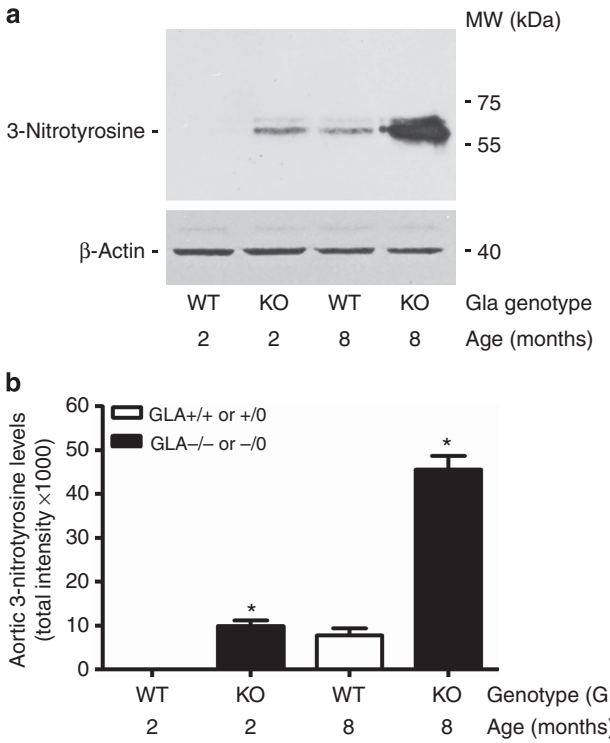

Figure 7 | Accumulation of protein-bound 3-nitrotyrosine in wild-type and Gla (alpha-galactosidase A) null mouse aortas. The detergent soluble proteins were extracted from clarified aortas. Equal amounts of lysate protein (100 μg) were subjected to a 6–13% gradient SDS-PAGE (sodium dodecyl sulfate-polyacrylamide gel electrophoresis) separation. The protein nitration in wild-type and Gla null mouse aortas was measured using a monoclonal antibody-specific for protein-bound nitrotyrosine. (**a**) A representative immunoblot image of protein-bound 3-nitrotyrosine (3NT) in mouse aortas. (**b**) The densitometric values were pooled from three immunoblot experiments using total 12 mice (four groups) at either 2 or 9 months of age. The data represent the mean ± s.e. ($n = 3$) for each group. *$P < 0.01$.

A more than sixfold elevation in 3NT concentration was observed in the Fabry cohort compared with the age-matched controls. No significant differences in the concentrations of chlorotyrosine, dityrosine, or ortho- or meta-tyrosine were measured between the two groups (Figure 8 and Table 2). No correlation was observed between the 3NT levels and the eGFRs, ages, plasma Gb3, or plasma lyso-Gb3 levels of the Fabry group (Supplementary Figures S1–S3 online). These measurements are consistent with eNOS uncoupling and resultant elevated reactive nitrogen species in untreated patients with classical FD.

DISCUSSION

Milestones in FD research included the discovery of the lysosome by de Duve and Wattiaux,[11] the recognized loss of GLA activity by Kint,[12] and the association of lysosomal inclusions in endothelial cells and smooth muscle cells of the vasculature by Hashimoto *et al.*[13] Subsequent work by Sweeley and Klionsky[14] and Brady *et al.*[15] documented that

Table 1 | Fabry disease and control patient characteristics

	Fabry disease *n* (%) or median (range)	Controls *n* (%) or median (range)
Males	13 (100)	11 (100)
Age	42.7 (16.8–53.7)	49.4 (20.4–60.5)
AGAL-A activity %	0.05 (0–2.8)	ND
GLA mutations		
Missense	5	
Nonsense, frame	6	
Shift/splice site	2	
Plasma Gb3	6.3 (5.3–9.74) $n=10$	ND
Lyso-Gb3	82.3 (152.7–150.3) $n=9$	ND
Age of diagnosis (year)	21.5 (12–41)	
Classical symptoms		
Acroparesthesia	12	
Cornea verticillata	12 ($n=12$)	
Angiokeratoma	11	
Organ involvement		
eGFR	95.5 (26–152)	99.8 (83–126)
LVH	5 ($n=12$)	ND
Stroke/TIA	3	0
Myocardial infarct/ CABG	0	0
ACE/ARB use	3	0
Cardiovascular risk factors		
Diabetes mellitus	0	0
Hypertension	3 ($n=12$)	1
Dyslipidemia	0	1
Smoking	5 ($n=12$)	3
Obesity	0	2

Abbreviations: ACE, angiotensin I converting enzyme inhibitor; AGAL-A, alpha-galactosidase A activity (relative to the mean reference value in healthy controls in leucocytes); ARB, angiotensin II receptor blockers; CABG, coronary artery bypass graft; eGFR, estimated glomerular filtration rate; GLA, alpha-galactosidase A; LVH, left ventricular hypertrophy; Lyso-Gb3, globotriaosylsphingosine; ND, not determined; TIA, transient ischemic attack.
Age and eGFR were not significantly different between Fabry and control groups based on a non-parametric *t*-test was used.

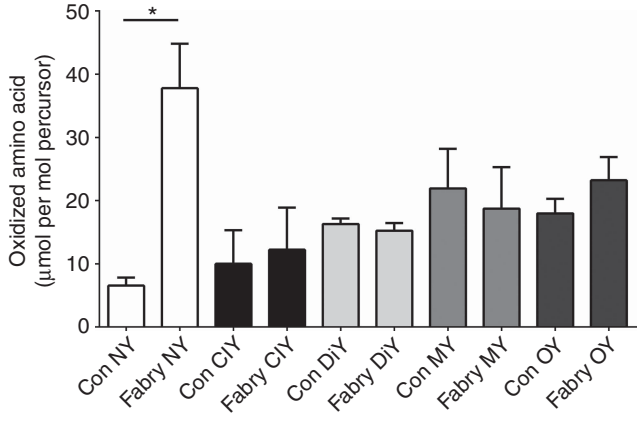

Figure 8 | Oxidized amino-acid levels in the plasma of classical Fabry patients and matched controls. The oxidized amino acids in the plasma were measured using liquid chomatography electron spray ionization mass spectrometry. The results were normalized to precursor amino-acid content and statistically analyzed using the Prism software. *$P<0.01$.

Table 2 | Plasma oxidized amino acid concentrations

	Fabry disease ($n=13$)	Controls ($n=11$)
3-Nitrotyrosine	37.8 (13.6–86.0)*	6.5 (1.7–14.0)
Chlorotyrosine	12.2 (0.03–74.5)	10.0 (0.04–50.3)
Dityrosine	15.2 (12.6–19.5)	16.3 (12.9–21.0)
Meta-tyrosine	18.7 (0.1–68.3)	21.9 (0.01–72.9)
Ortho-tyrosine	23.2 (9.6–49.7)	18.0 (7.4–86.1)

The oxidized amino-acid concentrations were assayed as described in the Materials and Methods section. The data are expressed as μmol/mmole of total protein tyrosine and represent medians (range) of triplicate assays performed twice per sample. *$P<0.01$.

the disease was due to a deficiency of GLA with the accumulation of globo series glycosphingolipids.

The use of recombinant GLA as enzyme replacement therapy is the standard of care for the treatment of FD. For several reasons, the benefits of enzyme replacement therapy for FD have been difficult to prove.[16,17] First, the time from diagnosis to a clinically meaningful outcome for FD is long. Decades often pass from the onset of symptoms before significant events such as stroke or renal failure occur. Second, study populations have usually been small, including patients in different disease stages. Finally, there are a limited number of biomarkers of FD and none are yet proven to be directly related to the pathogenesis of the vasculopathy. Establishing a mechanism for the vascular disease and subsequently a nexus between a biomarker and the progression of the vasculopathy would clearly be a valuable advance in the prospective management of these patients.

Two primary hypotheses have been proposed for the pathogenesis of the vasculopathy of FD. The first hypothesis proposes that circulating lyso-Gb3 deposits in the medial layer of the arterial vasculature promoting smooth muscle cell proliferating and modeling of the subendothelial layer. A resultant increase in shear stress results in increased expression of angiotensin receptors with subsequent formation of reactive oxygen species and NF-κB activation. These changes then lead to a decrease in NO synthesis and increase in β-integrin expression. The basis for this hypothesis has been recently reviewed.[18]

An alternative hypothesis proposes that eNOS dysregulation is the causal basis for Fabry-associated vasculopathy and that Gb3 accumulation in the endothelium alone is sufficient to account for the dysregulation of eNOS with lower NO bioavailability and eNOS uncoupling with the formation of reactive oxidants. This hypothesis is supported by the identification of three inducible models of vasculopathy in the Gla knockout mouse. When arterial injury was induced by the release of reactive oxygen species using rose Bengal, Gla knockout mice exhibited a highly robust sensitivity to carotid thrombosis.[2] This sensitivity correlated with the age of the mice as well as arterial Gb3 deposition. In another model, Gla knockout mice were bred on an apoE1-deficient background. Forty-five-week-old mice demonstrated a marked increase in atherosclerosis compared with Gla mice on a normal background.[3] In a third model, aortic rings from

wild-type and Gla null mice were pre-contracted with phenylephrine. The Gla-deficient rings demonstrated impaired relaxation to acetylcholine.[4] The defect was eliminated with calcium ionophore-stimulated endothelial relaxation, consistent with an abnormality in the plasma membrane of the endothelium. Primary cultures of aortic endothelial cells were employed to further document that increased plasma membrane Gb3 was the basis for the abnormality.[19,20] The Gb3 content of Gla knockout endothelial cells was markedly elevated in the total plasma membrane as well as the caveolar fractions. This increase was associated with decreased eNOS expression, hormone-stimulated eNOS activity, and levels of high molecular weight caveolin-1 oligomers.[21] These observations were consistent with a role for Gb3 in the assembly of the signalsome within caveolae, including eNOS. These experimental models of thrombosis, atherogenesis, and impaired relaxation identify eNOS dysregulation as a likely basis for the inducible models of vasculopathy.

Clinical studies attempting to assess the role of NO have been less consistent but in aggregate support a role for eNOS dysregulation. For example, comparing flow-mediated dilation of the brachial artery in Fabry patients and healthy controls, two studies have documented decreased arterial flow in the Fabry group.[22,23] This finding was confirmed using venous occlusion plethysmography and superficial index finger skin blood flow using laser Doppler flowmetry.[24,25] In other studies, decreased coronary blood flow has been measured in Fabry patients.[26,27] However, another group has demonstrated increased forearm blood flow in FD with acetylcholine infusion that persisted even when eNOS was inhibited by L-NMMA.[28]

Studies on cerebral blood flow have also yielded conflicting results reporting either decreased[29] or enhanced flow.[30] These seemingly contradictory findings may potentially be explained by eNOS uncoupling with secondary oxidative stress, resulting in protein nitration. A potential role for eNOS uncoupling is supported by a study of skin microvascular endothelial cells in which Gb3 loading resulted in an increase in reactive oxygen species. Gb3 loading was also associated with an increase in the transcription of intercellular adhesion molecule 1, vascular cellular adhesion molecule 1, and E-selectin.[31]

The current study addressed whether induced changes in Gb3 content in an endothelial cell line would be sufficient to account for eNOS dysregulation. EA.hy926 cells were employed. Conditions suitable for the reproducible loss of GLA activity by siRNA were established, and the secondary accumulation of Gb3 was documented. Under these conditions, there was a decrease in eNOS activity consistent with the impaired formation of NO. Concurrently, eNOS uncoupling with reactive nitrogen species formation was observed as measured by the formation of 3NT but not of other tyrosine adducts. These changes were not observed when GBA activity was similarly depressed.

Previous studies have highlighted a role for plasma 3NT as a marker for established cardiovascular disease in humans.[32,33] To further establish whether 3NT might be a suitable marker of vasculopathy in FD, mouse plasma from GLA knockout and wild-type mice were assayed and compared. 3NT levels were markedly increased and were further elevated in older knockout mice. Parallel changes in 3NT were measured in the mouse aortas. The absence of significant increases in ortho-tyrosine, meta-tyrosine, dityrosine, and chlorotyrosine in mouse plasma or aortic samples from the Gla null mice suggests that eNOS uncoupling alone is sufficient to account for the reactive oxygen species formed.[34]

Finally, 3NT levels were measured in biobanked plasma samples from untreated patients with classic FD. A robust and statistically significant increase in 3NT concentrations was measured in the absence of comparable changes in other oxidized amino acids. These findings suggest that eNOS uncoupling is likely present in human GLA deficiency and is a potential biomarker that directly correlates with a functional vascular abnormality. This finding requires confirmation with prospective clinical studies involving larger numbers of patients, including those with non-classical forms of the disease. If elevated plasma 3NT levels reflect the degree of vascular involvement in FD, then future studies may better define the role for 3NT in establishing the prognosis of the disorder, the risk to patients for developing vascular complications, and possibly the efficacy of current therapies designed to reduce Gb3. Importantly, the ability to demonstrate eNOS uncoupling directly by the measurement 3NT in an *in vitro* endothelial cell culture model, the Gla knockout mouse, and in patients with FD also provides a platform for the identification of more effective therapies.

MATERIALS AND METHODS

Mice

Wild-type C57BL/6 and Gla-deficient Fabry mice were housed and genotyped as described previously.[5] Animal studies were conducted in accordance with the University of Michigan Committee on the Use and Care of Laboratory Animals.

Cell cultures

EA.hy926 cells were purchased from ATCC (Manassas, VA). EA.hy926 cells are a human umbilical cell line established by the fusion of primary human umbilical vein cells with a thioguanine-resistant clone of A549 cells.[9] EA.hy926 cells were maintained in complete growth medium consisting of Dulbecco's Modified Eagle Medium/F12 (1:1, v/v)/GlutaMAX (Life Technologies, Grand Island, NY), 10% fetal bovine serum, 100 U/ml penicillin, and 100 μg/ml streptomycin, and subcultured twice weekly at a ratio of 1:5.

RNA interference

Anti-human siRNA oligonucleotides were predesigned and synthesized by Origene Technologies (Rockville, MD). The ID numbers for GLA, GBA, and GAPDH siRNAs were SR301812, SR301748, and SR301734, respectively. Each siRNA kit contained three Dicer-substrate 27-mer duplexes (dsiRNA). Stock concentrations of the siRNAs were made at 20 μM in RNase-free reconstitution buffer consisting of 100 mM potassium acetate and 30 mM HEPES (pH 7.5). Reconstituted siRNAs were heated at 94 °C for

2 min and then cooled to room temperature before storage at −20 °C.

One day before siRNA transfection, 8×10^5 EA.hy926 cells were seeded into a 100-mm culture dish containing 8 ml of complete growth medium. The transfection mixture was prepared immediately before addition. Briefly, LipofectamineRNAiMAX (Life Technologies) was diluted into 1 ml of Opti-MEM-I according to the manufacturer's guidelines, and the siRNA duplex was diluted with 1 ml of Opti-MEM-I at indicated final concentration. The dilution media were combined and incubated at room temperature for 20 min to form the siRNA/transfection reagent complex. The culture medium was replaced with 8 ml of Opti-MEM-I without serum and antibiotics, and the siRNA complex was gently dropped into the cell culture. After an 8-h transfection period, serum fetal bovine serum was added to attain a final concentration of 3%. On the second day of transfection, the Opti-MEM-I medium was replaced by complete growth medium. A second siRNA transfection was performed on day 4 following the first transfection as detailed above. The transfected EA.hy926 cells were harvested at the indicated days for immunoblotting, lipid, amino acid, or cell viability analyses.

Lipid analysis and western blotting

Glycosphingolipid analyses followed procedures previously described.[20] Immunoblot analysis of EA.hy926 cells followed previously published protocols.[5] For analysis of GLA knockdowns, rabbit anti-human GLA monoclonal antibody (LifeSpan BioSciences, Seattle, WA) was used at a dilution of 1:2500 (0.5 μg/ml). 3NT levels in mouse aortic lysates were analyzed with mouse anti-mouse 3NT monoclonal antibody (Abcam, Cambridge, MA) at a dilution of 1:2000 (0.4 μg/ml).

Analysis of oxidized amino acids

Cells or tissue samples were washed and homogenized in Buffer A consisting of 100 μM diethylenetetraminopentaacetic acid, 50 μM butylated hydroxytoluene, 10 μl/ml Halt protease inhibitor (Pierce, Rockford, IL) in 50 mM sodium phosphate buffer, pH 7.4. Homogenized cellular proteins were precipitated with ice-cold 10% trichloroacetic acid and delipidated with water/methanol/water-washed diethyl ether (1:3:7; vol/vol/vol). Known concentrations of isotopically labeled internal standards including $^{13}C_6$ tyrosine, $^{13}C_6$ phenylalanine and $^{13}C_6$ *ortho*-tyrosine, $^{13}C_6$ *o,o′*-dityrosine, $^{13}C_6$ 3NT and $^{13}C_6$ 3-chlorotyroine were added, and samples were hydrolyzed for 24 h in 4 N methane sulfonic acid supplemented with 1% benzoic acid. The hydrolysate was subjected to reverse-phase extraction with Supelclean ENVI ChromP columns (3 ml, Supelco, Bellefonte, PA). Oxidized amino acids were quantified using liquid chromatography–electrospray ionization tandem mass spectrometry in the multiple reaction monitoring mode as described previously.[5] The ratio of the peak areas of the analytes with corresponding $^{13}C_6$ internal standards were used to quantify levels of the analytes. Results were normalized to the content of tyrosine, the precursor of 3NT, 3-chlorotyrosine and *o,o*'-dityrosine, or to phenylalanine, the precursor for *ortho*- and *meta*-tyrosine.[35]

eNOS activity measurements

Cellular eNOS activities in control-siRNA and GLA-siRNA–transfected EA.hy926 cells were measured following an adopted protocol as described previously.[5]

Mouse tissue preparation

Mouse blood was withdrawn from the retro-orbital sinus using a Microvette EDTA-coated capillary blood collection tubes (Fisher Scientific, Pittsburgh, PA). The blood (120 μl) was immediately centrifuged at 1500×*g* for 15 min at 4 °C. Fifty microliter of plasma was recovered and stored at −80 °C for analysis of oxidized amino acids. Mouse aortas from wild-type and GLA null mice transfections were stored in antioxidant solution buffer A at −80 °C. Well-minced mouse aortas were homogenized with a Tissue Tearor (Biospec Products, Bartlesville, OK) and lysed in 1% Triton X-100 lysate buffer. The clarified aorta lysate was analyzed with the help of immunoblotting after BCA assay.

Human participants

Oxidized amino-acid levels were assayed from biobanked plasma samples from the Academic Medical Center in Amsterdam that included those from classical male FD patients. FD was diagnosed by GLA deficiency (defined as GLA activity <5% relative to the mean reference value in healthy controls) and by GLA genotyping[36] and the presence of elevated lyso-Gb3 levels.[37] Classical FD was defined as described in reference 38. Baseline plasma lyso-Gb3 and plasma Gb3 were previously determined as described in references[39] using reference values for lyso-Gb3 of 0.3–0.5 nmol/l and for plasma Gb3 of 1.08–3.18 μmol/l. Left ventricular hypertrophy was defined as an interventricular septal thickness in diastole of >12 mm. The glomerular filtration rate was estimated by CKD-EPI creatinine equation (eGFR). Plasma samples from 14 patients with classical FD were initially identified. However, one Fabry patient sample (with the highest measured 3NT) was excluded from the analysis upon determination that at the time of sampling the patient was recovering from cardiogenic shock with acute renal failure. The FD patients were age- and gender-matched to healthy controls, derived from an earlier study that included patient relatives with an excluded diagnosis of FD based on GLA genotyping, friends of the subjects, or subjects recruited by advertisement.[40] All FD and control subjects provided informed consent. The study conformed to the declaration of Helsinki and was conducted under institutional review board approvals at the Academic Medical Center of Amsterdam and the University of Michigan.

Statistical analysis

Cell data were analyzed using the Prism software (GraphPad, La Jolla, CA) using *t*-test or two-way analysis of variance and are expressed as mean ± s.e.m. Differences between control and treated samples were considered statistically significant at a *P*-value <0.05. Statistical analyses on patient samples were performed using SPSS. Constant variables are presented as medians (ranges). Differences between control and FD subjects were compared using non-parametric tests. Correlations between 3NT levels and patient characteristics were compared using Spearman's rank tests. $P<0.05$ was considered significant.

DISCLOSURE

JAS receives licensing royalties from Genzyme/Sanofi for eliglustat tartrate (Cerdelga) and related compounds. BES has received travel support from Shire HGT and Genzyme. CEMH and JMFGA have received honoraria for consultancies and speakers fees from Actelion, Genzyme, Shire HGT, and Protalix. All fees are donated to the Gaucher Stichting or the AMC Medical Research BV for research support. All the other authors declared no competing interests.

ACKNOWLEDGMENTS

This work was supported by the National Institutes of Health grant 5R01DK055823-13 (to JAS). Mass spectrometry experiments were performed in the University of Michigan Metabolomics Core (National Institutes of Health grants DK89503 and DK097153).

SUPPLEMENTARY MATERIAL

Figure S1. Relation of 3-nitrotyrosine levels and age in the plasma of classical Fabry patients and matched controls

Figure S2. Relation of plasma 3-nitrotyrosine levels and estimated glomerular filtration rate (eGFR) of classical Fabry patients and matched controls

Figure S3. Relation of plasma 3-nitrotyrosine levels and lyso-Gb3 concentration in Fabry patient plasma

Supplementary material is linked to the online version of the paper at http://www.nature.com/ki

REFERENCES

1. El Dib RP, Nascimento P, Pastores GM. Enzyme replacement therapy for Anderson-Fabry disease. *Cochrane Database Syst Rev* 2013; **2**: CD006663.
2. Eitzman DT, Bodary PF, Shen Y *et al.* Fabry disease in mice is associated with age-dependent susceptibility to vascular thrombosis. *J Am Soc Nephrol* 2003; **14**: 298–302.
3. Bodary PF, Shen Y, Vargas FB *et al.* Alpha-galactosidase A deficiency accelerates atherosclerosis in mice with apolipoprotein E deficiency. *Circulation* 2005; **111**: 629–632.
4. Park JL, Whitesall SE, D'Alecy LG *et al.* Vascular dysfunction in the alpha-galactosidase A-knockout mouse is an endothelial cell-, plasma membrane-based defect. *Clin Exp Pharmacol Physiol* 2008; **35**: 1156–1163.
5. Shu L, Park JL, Byun J *et al.* Decreased nitric oxide bioavailability in a mouse model of Fabry disease. *J Am Soc Nephrol* 2009; **20**: 1975–1985.
6. Shaul PW. Regulation of endothelial nitric oxide synthase: location, location, location. *Annu Rev Physiol* 2002; **64**: 749–774.
7. Kietadisorn R, Juni RP, Moens AL. Tackling endothelial dysfunction by modulating NOS uncoupling: new insights into its pathogenesis and therapeutic possibilities. *Am J Physiol Endocrinol Metab* 2012; **302**: E481–E495.
8. Edgell CJ, Haizlip JE, Bagnell CR *et al.* Endothelium specific Weibel-Palade bodies in a continuous human cell line, EA.hy926. *In Vitro Cell Dev Biol* 1990; **26**: 1167–1172.
9. Edgell CJ, McDonald CC, Graham JB. Permanent cell line expressing human factor VIII-related antigen established by hybridization. *Proc Natl Acad Sci USA* 1983; **80**: 3734–3737.
10. Ischiropoulos H. Biological tyrosine nitration: a pathophysiological function of nitric oxide and reactive oxygen species. *Arch Biochem Biophys* 1998; **356**: 1–11.
11. De Duve C, Wattiaux R. Functions of lysosomes. *Annu Rev Physiol* 1966; **28**: 435–492.
12. Kint JA. Fabry's disease: alpha-galactosidase deficiency. *Science* 1970; **167**: 1268–1269.
13. Hashimoto K, Gross BG, Lever WF. Angiokeratoma Corporis Diffusum (Fabry). Histochemical and electron microscopic studies of the skin. *J Invest Dermatol* 1965; **44**: 119–128.
14. Sweeley CC, Klionsky B. Fabry's Disease: Classification as a Sphingolipidosis and Partial Characterization of a Novel Glycolipid. *J Biol Chem* 1963; **238**: 3148–3150.
15. Brady RO, Gal AE, Bradley RM *et al.* Enzymatic defect in Fabry's disease. Ceramidetrihexosidase deficiency. *N Engl J Med* 1967; **276**: 1163–1167.
16. Wilcox WR, Banikazemi M, Guffon N *et al.* Long-term safety and efficacy of enzyme replacement therapy for Fabry disease. *Am J Hum Genet* 2004; **75**: 65–74.
17. Germain DP, Waldek S, Banikazemi M *et al.* Sustained, long-term renal stabilization after 54 months of agalsidase beta therapy in patients with Fabry disease. *J Am Soc Nephrol* 2007; **18**: 1547–1557.
18. Rombach SM, Twickler TB, Aerts JM *et al.* Vasculopathy in patients with Fabry disease: current controversies and research directions. *Mol Genet Metab* 2010; **99**: 99–108.
19. Shu LM, Murphy HS, Cooling L *et al.* An *in vitro* model of Fabry disease. *J Am Soc Nephrol* 2005; **16**: 2636–2645.
20. Shu L, Shayman JA. Caveolin-associated accumulation of globotriaosylceramide in the vascular endothelium of alpha-galactosidase A null mice. *J Biol Chem* 2007; **282**: 20960–20967.
21. Shu L, Shayman JA. Glycosphingolipid mediated caveolin-1 oligomerization. *J Glycomics Lipidomics* 2012; **S2**: 1–6.
22. Kalliokoski RJ, Kalliokoski KK, Penttinen M *et al.* Structural and functional changes in peripheral vasculature of Fabry patients. *J Inherit Metab Dis* 2006; **29**: 660–666.
23. Puccio D, Coppola G, Corrado E *et al.* Non invasive evaluation of endothelial function in patients with Anderson-Fabry disease. *Int Angiol* 2005; **24**: 295–299.
24. Stemper B, Hilz MJ. Postischemic cutaneous hyperperfusion in the presence of forearm hypoperfusion suggests sympathetic vasomotor dysfunction in Fabry disease. *J Neurol* 2003; **250**: 970–976.
25. Seino Y, Vyden JK, Philippart M *et al.* Peripheral hemodynamics in patients with Fabry's disease. *Am Heart J* 1983; **105**: 783–787.
26. Kalliokoski RJ, Kalliokoski KK, Sundell J *et al.* Impaired myocardial perfusion reserve but preserved peripheral endothelial function in patients with Fabry disease. *J Inherit Metab Dis* 2005; **28**: 563–573.
27. Dimitrow PP, Krzanowski M, Undas A. Reduced coronary flow reserve in Anderson-Fabry disease measured by transthoracic Doppler echocardiography. *Cardiovasc Ultrasound* 2005; **3**: 11.
28. Altarescu G, Moore DF, Pursley R *et al.* Enhanced endothelium-dependent vasodilation in Fabry disease. *Stroke* 2001; **32**: 1559–1562.
29. Hilz MJ, Kolodny EH, Brys M *et al.* Reduced cerebral blood flow velocity and impaired cerebral autoregulation in patients with Fabry disease. *J Neurol* 2004; **251**: 564–570.
30. Moore DF, Altarescu G, Ling GS *et al.* Elevated cerebral blood flow velocities in Fabry disease with reversal after enzyme replacement. *Stroke* 2002; **33**: 525–531.
31. Shen JS, Meng XL, Moore DF *et al.* Globotriaosylceramide induces oxidative stress and up-regulates cell adhesion molecule expression in Fabry disease endothelial cells. *Mol Genet Metab* 2008; **95**: 163–168.
32. Pennathur S, Bergt C, Shao B *et al.* Human atherosclerotic intima and blood of patients with established coronary artery disease contain high density lipoprotein damaged by reactive nitrogen species. *The J Biol Chem* 2004; **279**: 42977–42983.
33. Shishehbor MH, Aviles RJ, Brennan ML *et al.* Association of nitrotyrosine levels with cardiovascular disease and modulation by statin therapy. *JAMA* 2003; **289**: 1675–1680.
34. Heinecke JW. Oxidized amino acids: culprits in human atherosclerosis and indicators of oxidative stress. *Free Radic Biol Med* 2002; **32**: 1090–1101.
35. Vivekanandan-Giri A, Byun J, Pennathur S. Quantitative analysis of amino Acid oxidation markers by tandem mass spectrometry. *Methods Enzymol* 2011; **491**: 73–89.
36. Mayes JS, Scheerer JB, Sifers RN *et al.* Differential assay for lysosomal alpha-galactosidases in human tissues and its application to Fabry's disease. *Clin Chim Acta* 1981; **112**: 247–251.
37. Aerts JM, Groener JE, Kuiper S *et al.* Elevated globotriaosylsphingosine is a hallmark of Fabry disease. *Proc Natl Acad Sci USA* 2008; **105**: 2812–2817.
38. van der Tol L, Smid BE, Poorthuis BJ *et al.* A systematic review on screening for Fabry disease: prevalence of individuals with genetic variants of unknown significance. *J Med Genet* 2013, e-pub ahead of print; doi:10.1136/jmedgenet-2013-101857.
39. Gold H, Mirzaian M, Dekker N *et al.* Quantification of globotriaosylsphingosine in plasma and urine of fabry patients by stable isotope ultraperformance liquid chromatography-tandem mass spectrometry. *Clin Chem* 2013; **59**: 547–556.
40. Rombach SM, van den Bogaard B, de Groot E *et al.* Vascular aspects of Fabry disease in relation to clinical manifestations and elevations in plasma globotriaosylsphingosine. *Hypertension* 2012; **60**: 998–1005.